

# Thermoelectric Properties of Layer-Antiferromagnet CuCrS<sub>2</sub>

GIRISH C. TEWARI,<sup>1</sup> T.S. TRIPATHI,<sup>1</sup> and A.K. RASTOGI<sup>1,2</sup>

1.—School of Physical Sciences, Jawaharlal Nehru University, New Delhi 110067, India.  
2.—e-mail: akr0700@mail.jnu.ac.in

We have performed a detailed study of the electrical and thermal conductivities and thermoelectric power behavior of an antiferromagnetic-layer compound of chromium, CuCrS<sub>2</sub>, from 15 K to 300 K. Unlike previous studies, we find noninsulating properties and sensitive dependence on the preparation method, the microstructure, and the flaky texture formed in polycrystalline samples after extended sintering at high temperatures. Flakes are found to be metallic, with strong localization effects in the conductivity on cooling to low temperatures. The antiferromagnetic transition temperature  $T_N$  (=40 K) remains essentially unaffected. The Seebeck coefficient is found to be in the range of 150  $\mu\text{V/K}$  to 450  $\mu\text{V/K}$ , which is exceptionally large, and becomes temperature independent at high temperatures, even for specimens with low resistivity values of 5 m $\Omega$  cm to 200 m $\Omega$  cm. We find the thermal conductivity  $\kappa$  to be low, viz. 5 mW/K cm to 30 mW/K cm. This can be attributed mostly to the dominance of lattice conduction over electronic conduction. The value of  $\kappa$  is further reduced by disorder in Cu occupancy in the quenched phase. We also observe an unusually strong dip in  $\kappa$  at  $T_N$ , which is probably due to strong magnetocrystalline coupling in these compounds. Finally we discuss the properties of CuCrS<sub>2</sub> as a heavily doped Kondo-like insulator in its paramagnetic phase. The combination of the electronic properties observed in CuCrS<sub>2</sub> makes it a potential candidate for various thermoelectric applications.

**Key words:** Electrical and thermal conduction in crystalline metals and alloys, scattering mechanisms and Kondo effect, transition-metal compounds, thermoelectric materials

## INTRODUCTION

The ternary compounds of chromium, the cubic thiospinels  $\text{ACr}_2\text{X}_4$  ( $\text{A} = \text{Cu, Zn, Cd, or Hg; X} = \text{S, Se, or Te}$ ) and structurally related hexagonal layered  $\text{ACrX}_2$  ( $\text{A} = \text{Li, Na, K, Cu, or Ag}$ ) of the present study, have been extensively investigated for their magnetic properties.<sup>1–3</sup> In these compounds, magnetic interactions have an important effect on the electronic transport. The Cr thiospinels are well-known magnetic semiconductors. However, among these, the compounds containing Cu, i.e., CuCr<sub>2</sub>S<sub>4</sub> (Se<sub>4</sub>, Te<sub>4</sub>) are metallic with high values of ferromagnetic ordering temperature  $T_C$  of 420 K, 460 K, and 365 K, respectively. The metallic nature and the ferromagnetic behavior of these compounds

have been explained in terms of intermediate valency of Cr atoms,<sup>1,4,5</sup> which leads to a double exchange mechanism, as proposed by Zener.

The hexagonal layered compounds of Cr, including CuCrS<sub>2</sub> (Se<sub>2</sub>), are antiferromagnetic. The ordering temperatures  $T_N$  in these compounds are low (20 K to 55 K) despite the strong magnetic interactions, as can be deduced from the high value of the Curie–Weiss (CW) temperature  $\theta_{\text{CW}}$ , which varies from +250 K for  $\text{KCrSe}_2$ <sup>6,7</sup> to –250 K for LiCrS<sub>2</sub><sup>8,9</sup> in their paramagnetic phases.  $\theta_{\text{CW}}$  is related to the Cr–Cr distances within the hexagonal layer, and its strong variation in different compounds has been attributed to competing interactions between the direct antiferromagnetic and ferromagnetic superexchange through anion. The low value of  $T_N$  is due to weak antiferromagnetic interactions between successive Cr layers through the intervening Cu layer. This interpretation

assumes a localized and insulating nature of electrons of Cr<sup>3+</sup> ions that have spin-only moment of 3.9  $\mu_B$  for  $d^3$  configuration. Our present study, however, shows noninsulating properties and does not support a purely localized picture of the exchange interactions in these compounds. Moreover, neutron scattering studies have revealed that the ordered Cr moments are about 20% less than the expected value of 3.9  $\mu_B$  and that the direction of the moment is modulated, with the modulating vectors depending on the Cr–Cr distances in the different compounds. Successive planes in all of these compounds are coupled antiferromagnetically.<sup>8–10</sup>

The electronic transport properties of CuCrS<sub>2</sub> and CuCrSe<sub>2</sub> have not been investigated in detail. A preliminary conductivity measurement on crystals of CuCrS<sub>2</sub> by Le Nagard et al.<sup>11</sup> indicated semiconducting behavior. They found an unusually low activation energy  $E_{act}$  of around 4 meV in the temperature range from 60 K to 300 K and large conductivity at lower temperatures, thereby indicating noninsulating properties. Another study suggested that CuCrS<sub>2</sub> is a nonstoichiometric semiconductor and exhibits a changeover from *p*-type to *n*-type behavior when prepared under reduced sulfur vapor pressure and at higher temperatures.<sup>12</sup> This study was performed at temperatures above 600°C, so their conclusions are not applicable for the low-temperature transport properties. Moreover, Cu(Ag)CrS<sub>2</sub> also shows an order–disorder transition of Cu atoms around 400°C that may affect the electronic transport properties at high temperatures.<sup>8,9</sup> Apart from these studies, Cu(Ag)CrS<sub>2</sub> has also been characterized as a mixed ion–electron conductor. A large diffusion ionic conductivity of Cu<sup>+1</sup> ions on tetrahedral sites was measured above room temperature.<sup>13</sup> As far as electronic conductivity is concerned, one study found very large resistivity  $\sim 10^4 \Omega \text{ cm}$ , and the other an immeasurable high resistivity in CuCrS<sub>2</sub> at room temperature.<sup>14,15</sup>

We have measured the electronic transport properties of CuCrS<sub>2</sub> prepared by different methods. The dependence of the electronic transport properties of CuCrS<sub>2</sub> on temperature and crystalline quality are found to be qualitatively different from the previous studies mentioned above. We also report, for the first time, the results of thermoelectric power and thermal conductivity measurements on these compounds. The combination of our results shows that these compounds are potential candidates for various thermoelectric applications.

## PREPARATION AND CHARACTERIZATION

The compounds were prepared directly from reaction of elements Cu (99.9%), Cr (99.9%), and S (99.9%) and also from a diffusive reaction of a homogenized and compressed mixture of their binary compounds CuS (99+%) and Cr<sub>2</sub>S<sub>3</sub> (99%) in evacuated and sealed quartz tubes. We used CuS instead of the more stable Cu<sub>2</sub>S used in previous

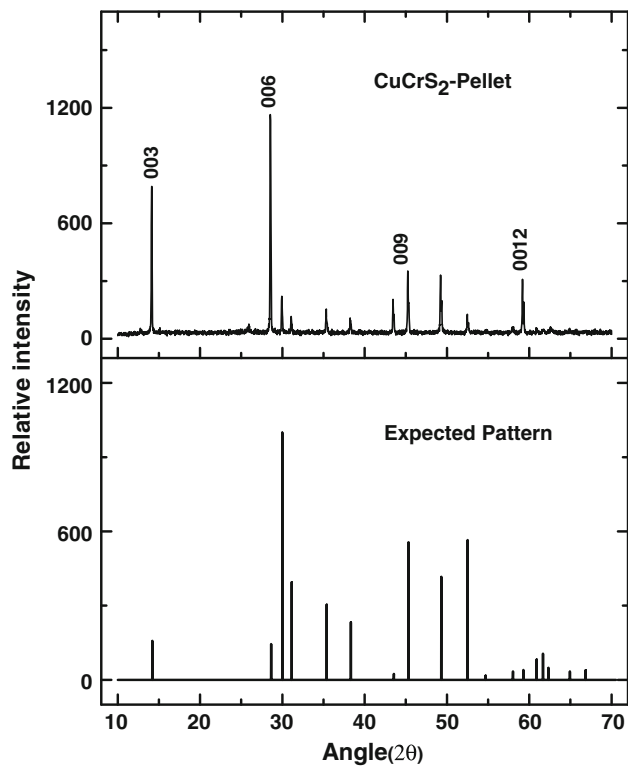


Fig. 1. X-ray diffraction pattern from the surface of a polycrystalline pellet prepared by sintering above 850°C over an extended period. Compared with the powder pattern<sup>11</sup> it shows increased intensity of (00l) reflections due to the flaky texture of the surface of the pellet.

studies<sup>11,14,15</sup> and carried out a very slow diffusive reaction of a compressed mixture of binaries at a lower temperature of about 650°C for 5 days. This procedure was adopted to avoid formation of the ferromagnetic phase CuCr<sub>2</sub>S<sub>4</sub>. The excess sulfur used in this method was separated and deposited at the cold end of the tube. The layered compounds Cu<sub>x</sub>CrS<sub>2</sub> ( $x = 0.9$  or 0.8), free from ferromagnetic spinel inclusions, could also be prepared by this method by varying the amount of CuS in the starting mixture. Regrinding, pelletizing under 5-ton pressure, and annealing at 850°C were necessary to obtain strain-free homogeneous final products. Some pellets were quenched from 850°C in air (samples 1 and 2), whereas others were cooled slowly (sample 3) to room temperature to obtain quenched, annealed phases of the respective compositions. The extended period of sintering at high temperature gave highly textured pellets (samples 1, 2, and 3) with growth of crystal flakes parallel to the surface of the pellets, as can easily be seen from the x-ray diffraction pattern (Fig. 1). On the other hand, the texturing was absent in phases which were synthesized by diffusive reaction of CuS and Cr<sub>2</sub>S<sub>3</sub> (samples 4 and 5).

Single-crystal flakes of sizes  $\sim 5 \text{ mm} \times 5 \text{ mm} \times 0.05 \text{ mm}$  were obtained along the lower-temperature end of a long tube that was kept at a temperature of 700°C to 800°C for 3 days to 4 days. We have

detected approximately 3% to 4% ferromagnetic impurity phase in the flakes and powders, when prepared at lower temperatures and by using excess amount of sulfur. The magnetic impurities were significantly reduced to less than 1% in our flakes after re-annealing them at 850°C for 4 h to 5 h in a running vacuum of 10<sup>-2</sup> mmHg. The phases obtained at high temperature were found to be cation rich. A typical atomic ratio of Cu:Cr:S was found to be 1.08:1.07:2 based on energy-dispersive x-ray analysis (EDAX). We could not ascertain the off-stoichiometry of our flakes, because of small inclusions of the magnetic phase in them.

### X-Ray Diffraction

The compounds prepared by different methods [quenched, annealed specimen as well as Cu<sub>x</sub>CrS<sub>2</sub> ( $x = 0.8$  or  $0.9$ )] gave sharp peaks in the x-ray diffraction pattern without any significant change in the cell parameters from the values reported previously by Le Nagard et al.<sup>11</sup> for the crystals. We also support their conclusion that a large disorder in the Cu occupancy in this compound cannot be quenched below the ordering transition at 400°C, since no discernible changes in x-ray peaks were noticed by rapid cooling through the transition.

### Flaky Texture

Figure 1 shows an x-ray pattern recorded by using reflections directly from the surface of a pellet sintered over a long period of 5 days at 850°C. We compare this pattern with the pattern shown in Fig. 1 expected for randomly oriented crystallites of its powder.<sup>11</sup> The increased intensity of all the (00l) reflections shows the flaky texture of the surface of the pellet. We will see below that this texturing has significant effects on the transport properties of the pellets.

## MAGNETIC PROPERTIES

The magnetic susceptibility  $\chi$  of CuCrS<sub>2</sub> from 2 K to 300 K at 500 Oe field, and the magnetization (inset to Fig. 2) up to 14 T field at 2 K, are plotted in Fig. 2.  $\chi$  follows a CW dependence:  $\chi = C/(T + \theta)$ , with  $C = 1.9$  emu/mole and  $\theta = 110$  K, above 200 K (continuous line in Fig. 2). The  $C$  value corresponds to an effective moment of 3.9  $\mu_B/\text{Cr}$ , as expected for total spin 3/2 for its  $d^3$  configuration and with the quenched orbital contribution. The susceptibility  $\chi$  starts deviating from the CW dependence below 200 K on cooling toward the magnetic transition at  $T_N = 40.5$  K. The magnetization in the antiferromagnetic phase at 2 K up to 14 T field is plotted in the inset to Fig. 2; it shows an upward curvature at high fields. This  $M(H)$  dependence confirms the helicoidal order of Cr moments, earlier deduced from neutron scattering measurements.<sup>10</sup> Significantly, neutron scattering also yielded moments of the Cr atoms that were about 20% smaller in the ordered phase than the value expected for spin 3/2

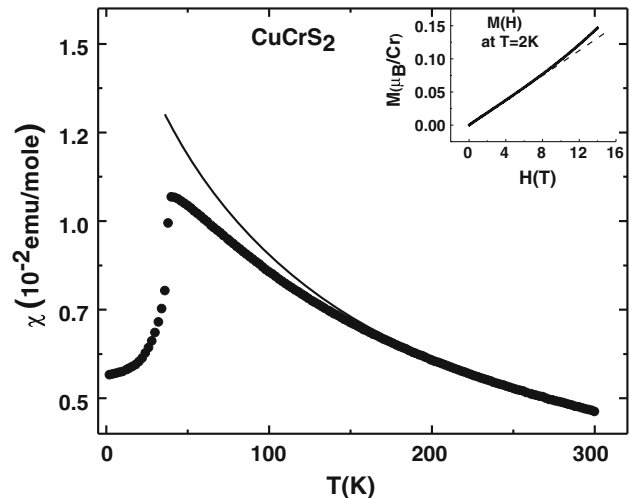


Fig. 2. Magnetic susceptibility  $\chi$  of CuCrS<sub>2</sub>, showing departure from CW dependence (continuous curve) below 200 K. The upward deviation of magnetization  $M$  at 2 K above 3 T field (shown in inset) indicates helicoidal order of Cr spins in the antiferromagnetic phase.

in its paramagnetic phase. There is no explanation available for the reduction of the Cr moments at low temperatures. In our opinion, the observation of fractional moments of Cr atoms in CuCrS<sub>2</sub> is quite significant and may be the consequence of the non-localized nature of their electrons, resulting from strong hybridization of the 3d orbital of Cr with the *sp* orbital of surrounding sulfur atoms.

## TRANSPORT PROPERTIES

### Experimental Procedures

Electrical conductivity measurements on sintered pellets and crystal flakes between 15 K and 300 K were performed by the four-probe method using silver paste for electrical contacts. The thermopower of the pellets and the crystal flakes was studied by measuring the Seebeck coefficient  $S$  ( $=\Delta V/\Delta T$ ) with respect to copper from 15 K to 300 K using a differential measurement method. In this method, at a stabilized temperature, a small temperature gradient is generated across the sample length, and the thermoelectric voltage is recorded using copper leads. The spurious and offset voltages of the measuring circuit were eliminated by reversing the temperature gradient and averaging the recorded voltages. The apparatus was tested for accuracy by measuring  $S$  on a thin piece of pure lead with respect to copper versus temperature.<sup>16</sup> The thermal conductivity  $\kappa$  at different temperatures was measured by passing a known heat current through the length of a rectangular piece of pellet and recording the temperature difference by using a Au (0.05%Fe)/Chromel differential thermocouple after steady state was reached. This method was tested by measuring the  $\kappa$  of a rectangular piece of sintered alumina substrate from 15 K to 300 K (shown in the inset to Fig. 5) and comparing it with the expected

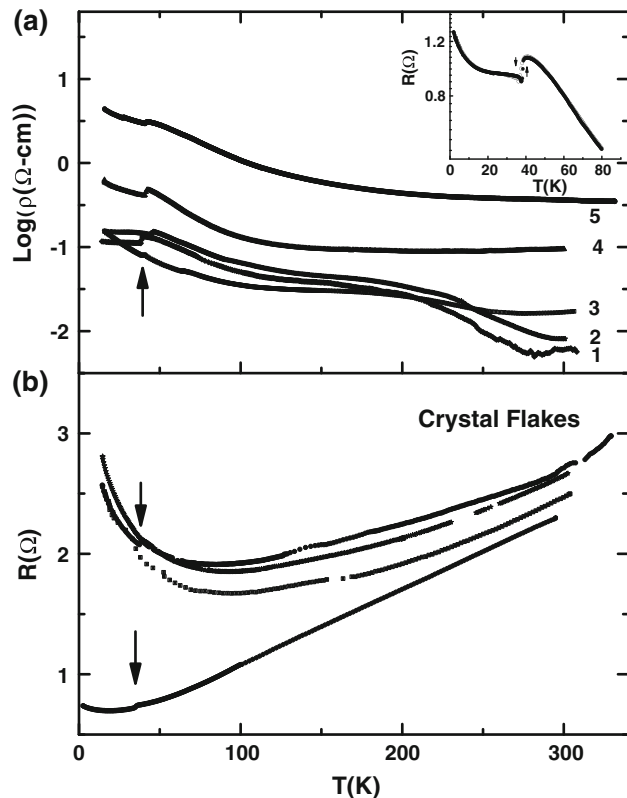


Fig. 3. (a) The resistivity dependence [plotted as  $\log(\rho)$  versus  $T$ ] of pellets of  $\text{CuCrS}_2$  prepared by different thermal treatments. The extended period of sintering at higher temperature (1, 2, and 3) and quenching (1 and 2) gives lower resistivity compared with the phases prepared from the binary compounds, including compounds  $\text{Cu}_{0.9}\text{CrS}_2$  (4) and  $\text{Cu}_{0.8}\text{CrS}_2$  (5). (b) Resistance of a few crystal flakes, showing a minimum below 100 K. Arrows mark the magnetic transition  $T_N$ . The anomaly with hysteresis at  $T_N$  is shown for one of the pellets in the inset to (a).

values.<sup>17</sup> The accuracy of thermopower and thermal conductivity values for our compounds is about 5%.

### Electrical Conductivity

In Fig. 3, we show the temperature dependence of the resistivity of different samples. The resistivity of

samples prepared directly from the elements (1, 2, and 3) and also from interdiffusion of binary compounds (4 and 5) is plotted as  $\log(\rho)$  in Fig. 3a, and the in-plane resistance of some of the crystal flakes is shown on a linear scale in Fig. 3b. The final heat treatment in the case of samples 1, 2, and 3 was sintering at 850°C to 900°C for 5 days, followed by quenching (1 and 2) or slow cooling (3). The pellets of all of them showed varying degrees of flaky texturing, as mentioned above. Sample 3 was prepared using 10% excess sulfur, and it contained a small amount (<2%) of ferromagnetic inclusions. Samples 4 and 5, with nominal composition  $\text{Cu}_{0.9}\text{CrS}_2$  and  $\text{Cu}_{0.8}\text{CrS}_2$ , respectively, were made by interdiffusion of binaries and annealing at 850°C for 2 days.

The resistances of all the polycrystalline pellets were measured parallel to their planes and were found to increase on cooling to low temperatures. Samples (1 and 2) with the maximum flaky texture had substantially lower resistivity at room temperature. A characteristic feature, viz. the plateau in their resistivity, can be seen to develop around 150 K to 200 K. This feature was absent in phases with larger resistances, which were prepared at lower temperatures, especially when using the interdiffusion route. We believe that the plateau-like feature in the resistance on cooling is a characteristic feature of the phases obtained after extended period of sintering at high temperature, which gives a high degree of flaky texture (Fig. 1) and substantially lower resistivity at room temperature. This behavior may be due to carrier doping and related to the as-yet unknown nature of localization by impurities on cooling in their cation-rich compositions. The resistivity values at 300 K for different samples are presented in Table I.

A common feature for all the samples, including Cu-deficient ones, is the noninsulating-like temperature dependence at low temperatures, as can be seen in Fig. 3. Although a significant increase in resistance on cooling toward magnetic transition is found, this increase is surely nonexponential.

**Table I. Properties of polycrystalline pellets and flakes of  $\text{CuCrS}_2$  at 300 K**

No.	Composition (Nominal Ratio)	Thermal Treatment <sup>a</sup>	$\rho$ (mΩ cm)	S (μV/K)	$\kappa$ (mW/K cm)	ZT <sup>c</sup>
1	$\text{CuCrS}_2$ (Cu + Cr + 2S)	Extended sintering (5 days) at 850°C + air quenched	6	445 <sup>b</sup>	4.8	2.0
2	$\text{CuCrS}_2$ (Cu + Cr + 2.1S)	Extended sintering (5 days) at 950°C + air quenched	8	276 <sup>b</sup>	5.4	0.53
3	$\text{CuCrS}_2$ (Cu + Cr + 2.2S)	Extended sintering (5 days) at 850°C + slowly cooled	15	170	6.5	0.1
4	$\text{Cu}_{0.9}\text{CrS}_2$ (0.9CuS + 0.5Cr <sub>2</sub> S <sub>3</sub> )	Sintered (2 days) at 900°C + air quenched	90	217	17	0.01
5	$\text{Cu}_{0.9}\text{CrS}_2$ (0.8CuS + 0.5Cr <sub>2</sub> S <sub>3</sub> )	Sintered (2 days) at 900°C + air quenched	350	176	—	—
6	Crystal flake	Excess S vapor (thickness ~20–30 μm)	8	185	—	—

<sup>a</sup>Packing density of the sintered pellets is about 80% to 85% of the theoretical value; <sup>b</sup>Pellets with large flaky texture; <sup>c</sup>ZT =  $S^2T/(\rho\kappa)$ .

The resistance at  $T_N$  becomes at most 10 to 20 times the room-temperature value, and then increases much more slowly at low temperatures in the anti-ferromagnetic phase. The resistivity at  $T_N$  exhibits a hysteretic anomaly, as can be seen in the inset to Fig. 3a. This confirms the first-order nature of this transition, which was also reported in a recent neutron scattering study.<sup>18</sup> They found a structural modification (rhombohedral to monoclinic) due to strong magnetocrystalline coupling in this compound, resulting in a first-order nature of the transition at  $T_N$ .<sup>18</sup> A previous study on the isostructural–isoelectronic compound AgCrS<sub>2</sub> also reported diffused first-order nature of the antiferromagnetic–paramagnetic phase transition at 42 K based on heat capacity measurements.<sup>19</sup>

The lower panel of Fig. 3 shows the resistance measured in-plane of the crystal flakes of CuCrS<sub>2</sub>. We find a metal-like dependence in all of them, and large variations in the resistivity of different flakes from 5 mΩ cm to 100 mΩ cm around room temperature. The resistance shows a small rise after it passes through a Kondo-like minimum below 100 K. The transitional anomaly as a downward jump in resistance at magnetic transition is also seen in some of the flakes. Our results clearly show that the resistivity behavior of CuCrS<sub>2</sub> is quite complex, and is unlike to a doped semiconductor as was suggested in earlier studies.<sup>11,14,15</sup>

### Thermopower

The most remarkable property of CuCrS<sub>2</sub> is the abnormally large value of the Seebeck coefficient  $S$  of our pellets and a crystal flake (Fig. 4). The samples obtained after extended sintering at high

temperatures (1, 2, and 3) have comparatively higher values of  $S$  with a maximum of 450 μV/K for the quenched phase. The compounds prepared through the interdiffusion route, Cu<sub>0.9</sub>CrS<sub>2</sub> (sample 4) and Cu<sub>0.8</sub>CrS<sub>2</sub> (sample 5), have comparatively smaller values, although  $S$  remain significantly large at 200 μV/K to 300 μV/K around room temperature. The room-temperature value of  $S$  for different samples is presented in Table I. The sign of  $S$  is positive for all samples, including the flakes. Moreover,  $S$  is found to vary smoothly across the magnetic transition temperature  $T_N$ ; it increases rapidly on heating above the magnetically ordered phase and saturates to a constant value in the paramagnetic phase above ~150 K.

### Thermal Conductivity

Figure 5 shows the thermal conductivity  $\kappa$  of different pellets as a function of temperature, plotted on a log( $T$ ) scale between 15 K and 300 K. The thermal conductivity of a sintered alumina substrate, measured for calibration of our apparatus, is shown in the inset to Fig. 5. The value of  $\kappa$  for different samples at room temperatures is quite different. This variation in  $\kappa$  value may partly be due to varying contributions of grain-boundary scattering of phonons due to the rather poor packing density (80% to 85% in our case) of the sintered pellets. The  $\rho$  and  $S$  behaviors of the same pellets are shown in Figs. 3 and 4. It is remarkable to find that, among them, the value of  $\kappa$  is substantially lower for the quenched phases (1 and 2), which have comparatively lower resistivity and larger thermopower at room temperature. We note that the contribution to the thermal conductivity in these compounds is

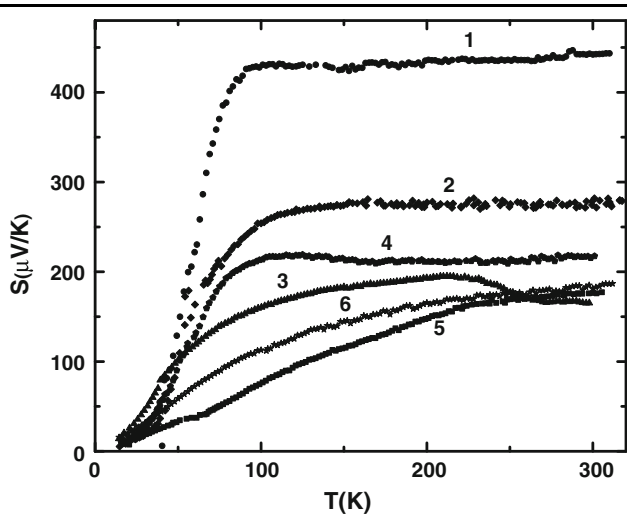


Fig. 4. The positive Seebeck coefficients  $S$  of different pellets and a crystal flake (6), showing large and constant values at high temperatures. The largest value of  $S$  is found for pellets showing the largest flaky texture. The temperature dependence of  $S$  is similar for the phases with Cu-deficient composition, Cu<sub>0.9</sub>CrS<sub>2</sub> (4) and Cu<sub>0.8</sub>CrS<sub>2</sub> (5).

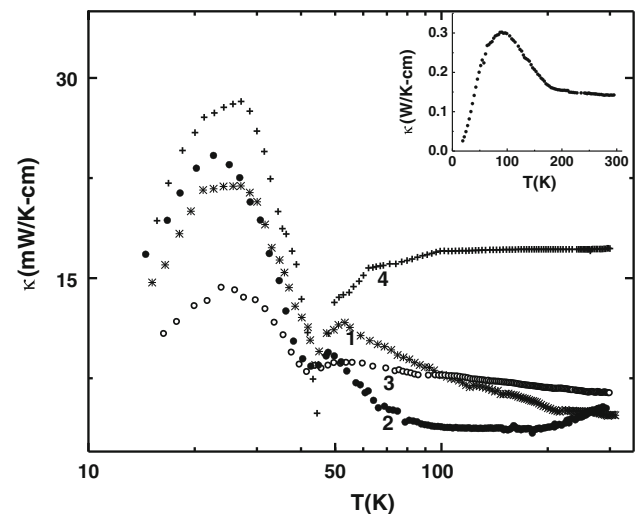


Fig. 5. Thermal conductivity  $\kappa$  of pellets plotted versus log( $T$ ) for the quenched (1 and 2), slowly cooled (3), and Cu<sub>0.9</sub>CrS<sub>2</sub> (4) samples. A strong dip in  $\kappa$  is seen near  $T_N$  in all of them. The  $\kappa$  value in the quenched phases (1 and 2) is reduced due to disorder in Cu occupancy. The  $\kappa$  measured on a thin, sintered rectangular alumina piece for calibration of the apparatus is presented in the inset.

mostly due to the atomic lattice. The electronic contribution, as estimated using the Lorenz number, accounts for less than 30% of the  $\kappa$  value at room temperature, even in the case of the most conducting pellets (1 and 2). Moreover, at low temperatures, the electronic contribution becomes insignificant in all the samples. The further reduction of  $\kappa$  value in the quenched phase may be the result of increased atomic disorder in the occupancy of Cu atoms.

An unusual and remarkably large effect of magnetic transition on the thermal conductivity can be seen in all the pellets. We find that  $\kappa$  shows a large dip as we approach the magnetic transition  $T_N$  from above as well as from below. We believe that the dip in  $\kappa$  is caused by unusually large magnetoelastic coupling<sup>18</sup> that gives rise to the first-order nature of the magnetic transition. As a result of the magnetoelastic coupling, short-range magnetic correlations cause strong scattering of the phonons, leading to a dip in  $\kappa$  as the magnetic transition is approached from the paramagnetic side. The thermal conductivity  $\kappa$  increases rapidly as soon as the magnetic order is set up. The strong reduction in  $\kappa$  seems also to be correlated with the reduction in electronic conduction (i.e., rise in resistivity; Fig. 3) on cooling as we approach the magnetic transition. It is interesting to note that, in this same temperature interval, the paramagnetic susceptibility also shows significant deviation from CW behavior, as can be seen from Fig. 2. These properties indicate the importance of magnetoelastic coupling for scattering of electrons and phonons by the short-range magnetic correlations which are built up much above  $T_N$  in these layered compounds and cause simultaneous variations in  $\chi$ ,  $\rho$ ,  $S$ , and  $\kappa$ , as observed herein.

## DISCUSSION

The resistances of all pellets increase on cooling, in the same manner as found by Le Nagard et al.<sup>11</sup> in the case of single crystals. Despite this increase, the resistivities at low temperatures remain quite small, indicating the noninsulating character of our compounds. We believe this to be an intrinsic property of these compounds. In this context, the observation of a minimum in the resistivity of the flakes (Fig. 3b) is quite significant, and indicates Kondo-type magnetic scattering of conduction electrons from the paramagnetic centers. This mechanism can also explain the unusually large Seebeck coefficient  $S$  at high temperatures. In the case of the Kondo model, the exchange interaction between localized paramagnetic centers and conduction electrons causes scattering which depends strongly on the energy of the conduction electrons, thus leading to anomalously large, temperature-independent thermopower at high temperatures. Our results also show that the qualitative behavior of the electronic transport is not greatly affected by

the change in carrier doping and the disorder in Cu occupancy in different metal-rich compositions obtained after long sintering at high temperatures and quenched through order-disorder transition.

The temperature dependence of the electrical conductivity together with the exceptionally high value of the thermopower in our compounds is very similar to that found in Kondo insulators, for example,  $\text{Ce}_3\text{Pt}_3\text{Sb}_4$ .<sup>20</sup> We therefore believe that a doped Kondo-insulator-like phase is realized in the paramagnetic phase of  $\text{CuCrS}_2$ . In a Kondo insulator, conduction electrons suffer a small hybridization gap due to the proximity of the nearly localized 4f energy levels of rare-earth atom, or 3d energy levels of Cr in our case. This causes a small excitation gap for the conduction of electrons and in turn is also responsible for their inelastic scattering by the magnetic fluctuation of localized electrons. Strong energy dependence of this scattering results in a high thermoelectric coefficient. However, in contrast to the nonmagnetic properties of Ce compounds, direct Cr-Cr magnetic interactions give rise to antiferromagnetic order in  $\text{CuCrS}_2$  at low temperatures.

In Kondo insulators, magnetic centers have unstable valency and show strong fluctuations of moments. From the observed CW dependence of the magnetic susceptibility, nearly integral valency of Cr atoms is deduced, which suggests highly localized spin fluctuations of the Cr atoms above 200 K. At lower temperatures,  $\chi$  deviates significantly from CW behavior, as can be seen in Fig. 2. Moreover, neutron diffraction study<sup>10</sup> yields about 20% reduced moment of Cr atoms than expected based on the spin-only 3/2 value. The reduction in magnetic moment of Cr atoms may imply efficient mixing of 3d electrons with valence electrons (or holes) of chalcogen atoms as the temperature is reduced. This mixing mechanism may be the reason behind the complex temperature dependence of the transport properties of  $\text{CuCrS}_2$ , as observed by us.

In contrast to the layered compound  $\text{CuCrS}_2$ , the related cubic thiospinels compounds  $\text{CuCr}_2\text{S}_4$  ( $\text{Se}_4$ ,  $\text{Te}_4$ ) show good metallic properties. In the latter compounds, Cr atoms are clearly in intermediate valence state, as was deduced from the Curie constant in their paramagnetic phase and also from the saturation magnetization in the ferromagnetic phase.<sup>5</sup> In addition, the behaviors of  $\rho$  and  $S$  in the metallic thiospinels are quite typical of d-band conductors, similar to transition-metal compounds such as ferromagnetic nickel.<sup>5</sup> The qualitative difference in the transport properties of the layered counterpart is basically due to the anisotropic structure and the smaller extent of broadening of the 3d band by hybridization with the valence band originating from the sulfur anions. This leads to strong localization effects due to disorder-induced scattering of conduction electrons. We have also carried out a detailed investigation of the properties of the corresponding layer-selenide compound

CuCrSe<sub>2</sub>, which is also antiferromagnetic below 55 K. Our measurements show that, compared with the sulfide, CuCrSe<sub>2</sub> shows good metallic conduction and lower thermopower, most probably due to increased hybridization broadening of 3d bands with the valence band of selenium in this compound.<sup>21</sup>

## CONCLUSIONS

We have prepared the layered compound CuCrS<sub>2</sub> by different heat treatments and report for the first time its thermoelectric power and thermal conductivity properties. A common feature of the transport properties of different samples is nonmetallic, non-insulating dependence of resistivity at low temperatures and an unusually large Seebeck coefficient around room temperature. We discuss this behavior in terms of doped Kondo-insulator-like phase in the paramagnetic phase of CuCrS<sub>2</sub>. We find an unusually small activation for conduction and a highly energy-dependent scattering of conduction electrons from the magnetic fluctuations, leading to anomalously large thermopower in CuCrS<sub>2</sub>. These properties combined with their poor thermal conductivity, which is further reduced by increased disorder in Cu occupancy in the quenched phases, make them potential candidates for various thermoelectric applications. These compounds also have large magnetocrystalline coupling. Consequently, both the conduction electrons and the phonons are strongly scattered by the correlated spin fluctuations of the Cr atoms on cooling toward the anti-ferromagnetic transition temperature. As a result of these scatterings the electrical conductivity as well as the thermal conductivity is found to decrease while approaching the magnetic transition temperature. A thorough study of the electronic structure and low-energy excitations in this interesting class of layered antiferromagnets would be quite rewarding.

## ACKNOWLEDGEMENTS

G.C. Tewari and T.S. Tripathi acknowledge the Council of Scientific and Industrial Research (CSIR) India. We deeply acknowledge the help and valuable suggestions of Dr G. Jeffrey Snyder, Materials

Science, California Institute of Technology, California. We also acknowledge Dr. Alok Banerjee UGC-DAE Consortium for Scientific Research (CSR), Indore, India for the magnetic measurements at the 14T facility.

## REFERENCES

1. R.P. Van Stapele, *Ferromagnetic Materials*, Vol. 3, ed. E.P. Wohlfarth (Amsterdam: North-Holland, 1982).
2. W. Bronger, *Crystallography and Crystal Chemistry of Materials with Layered Structures*, ed. F. Levy (Dordrecht: Reidel, 1976), pp. 93–125.
3. P.F. Bongers, C.F. Van Bruggen, J. Koopstra, W.P.F.A.M. Omloo, G.A. Wiegers, and F. Jellinek, *J. Phys. Chem. Solids* 29, 977 (1968).
4. F.K. Lotgering and R.P. Van Stapele, *J. Appl. Phys.* 38, 403 (1968).
5. T.S. Tripathi, G.C. Tewari, and A.K. Rastogi, *International Conference on Magnetism, ICM-2009* (We-HT4-04, 2009).
6. G.A. Wiegers, *Proceedings of the International Conference on Layered Materials and Intercalates*, ed. C.F. Van Bruggen, C. Haas, and H.W. Myron, *Physica* 99B, 151 (1980).
7. J. Dijkstra, C.F. Van Bruggen, and C. Haas, *Phys. Rev. B* 40, 7873 (1989).
8. F.M.R. Engelsman, G.A. Wiegers, F. Jellinek, and B. Van Laar, *J. Solid Status Chem.*, 6, 574 (1973).
9. B. Van Laar and D.J.W. Ijdo, *J. Solid State Chem.* 3, 590 (1971).
10. M. Wintenberger and Y. Allain, *Solid State Commun.* 64, 1343 (1987).
11. N. Le Nagard, G. Collin, and O. Gorochov, *Mater. Res. Bull.* 14, 1411 (1979).
12. M.A. Bouthila, J. Rasnuor, M.E.L. Aatmani, and H. Lyahyaoni, *J. Alloys Compd.* 283, 88 (1999).
13. G.M. Abramova, A.M. Vorotynov, G.A. Petrakovskii, N.I. Kiselev, D.A. Velikanov, A.F. Bovina, R.F. Al'mukhametov, R.A. Yakshibaev, and E.V. Gabitov, *Phys. Solid State* 46, 2245 (2004).
14. N. Tsujii, H. Kitazawa, and G. Kido, *Phys. Status Solidi (C)* 3, 2775 (2006).
15. N. Tsujii and H. Kitazawa, *J. Phys.: Condens. Matter*, 19, 145245 (2007).
16. F.J. Blatt, A. Schroeder, C.L. Foiles, and D. Greig, *Thermoelectric Power of Metals* (New York: Plenum, 1976).
17. N.P. Bansal, Zhu Dongming NASA/TM-2003-212896.
18. C.E. Rasch Julia, M. Boehm, C. Ritter, H. Mutka, J. Schefer, L. Keller, G. M. Abramova, A. Cervellino, and J.F. Loffler, *Phys. Rev. B* 80, 104431 (2009).
19. H. Kawaji, T. Atake, and Y. Saito, *J. Phys. Chem. Solids* 50, 215 (1989).
20. C.D.W. Jones, K.A. Regan, and F.J. DiSalvo, *Phys. Rev. B* 58, 16057 (1998).
21. G.C. Tewari, T.S. Tripathi, and A.K. Rastogi (under preparation).